frontiers in Sustainable Food Systems

ORIGINAL RESEARCH
published: 24 May 2021
doi: 10.3389/fsufs.2021.658592

Hydrothermal Liquefaction of Food Waste: Effect of Process Parameters on Product Yields and Chemistry

Hengameh Bayat[1], *Mostafa Dehghanizadeh*[1], *Jacqueline M. Jarvis*[2], *Catherine E. Brewer*[1] *and Umakanta Jena*[1]*

[1] Department of Chemical and Materials Engineering, New Mexico State University, Las Cruces, NM, United States,
[2] Department of Plant and Environmental Sciences, New Mexico State University, Las Cruces, NM, United States

Increasing food waste generation (1.6 billion tons per year globally) due to urban and industrial development has prompted researchers to pursue alternative waste management methods. Energy valorization of food waste is a method that can reduce the environmental impacts of landfills and the global reliance on crude oil for liquid fuels. In this study, food waste was converted to bio-crude oil *via* hydrothermal liquefaction (HTL) in a batch reactor at moderate temperatures (240–295°C), reaction times (0–60 min), and 15 wt.% solids loading. The maximum HTL bio-crude oil yield (27.5 wt.%), and energy recovery (49%) were obtained at 240°C and 30 min, while the highest bio-crude oil energy content (40.2 MJ/kg) was observed at 295°C. The properties of the bio-crude oil were determined using thermogravimetric analysis, fatty acid methyl ester (FAME) analysis by gas chromatography with flame ionization detection, CHNS elemental analysis, and ultrahigh-resolution Fourier transform ion cyclotron resonance mass spectroscopy (FT-ICR MS). FT-ICR MS results indicated that the majority of the detected compounds in the bio-crude oil were oxygen-containing species. The O_4 class was the most abundant class of heteroatom-containing compounds in all HTL bio-crude oil samples produced at 240°C; the O_2 class was the most abundant class obtained at 265 and 295°C. The total FAME content of the bio-crude oil was 15–37 wt.%, of which the most abundant were palmitic acid (C16:0), palmitoleic acid (C16:1), stearic acid (C18:0), and polyunsaturated fatty acids (C18:3N:3, C18:3N:6).

Keywords: food waste, bio-crude oil, combustion characteristics, high-resolution FT-ICR MS, hydrothermal liquefaction

OPEN ACCESS

Edited by:
Francisco Jesus Fernandez Morales, University of Castilla-La Mancha, Spain

Reviewed by:
Shicheng Zhang, Fudan University, China
Teresa Gea, Universitat Autònoma de Barcelona, Spain
Wan-Ting (Grace) Chen, University of Massachusetts Lowell, United States

***Correspondence:**
Umakanta Jena
ujena@nmsu.edu

Specialty section:
This article was submitted to Waste Management in Agroecosystems, a section of the journal Frontiers in Sustainable Food Systems

Received: *26 January 2021*
Accepted: *22 April 2021*
Published: *24 May 2021*

Citation:
Bayat H, Dehghanizadeh M, Jarvis JM, Brewer CE and Jena U (2021) Hydrothermal Liquefaction of Food Waste: Effect of Process Parameters on Product Yields and Chemistry. Front. Sustain. Food Syst. 5:658592. doi: 10.3389/fsufs.2021.658592

INTRODUCTION

Food wastes represent the largest fraction (21.6%) of the total generated municipal solid wastes, and are associated with several environmental, social, and economic problems. According to the U.S. Environmental Protection Agency (EPA), 63.1 million tons of food was wasted in the U.S in 2018, ∼22.4 million tons more than the amount generated in 2017 (U.S.E.P.A., 2020b). Decomposing wet food waste in landfills produces uncontrolled methane (CH_4) and carbon dioxide (CO_2), making landfills the third largest source of CH_4 emissions in the U.S. (∼17% of the total methane emissions) (U.S.E.P.A., 2020a). Leachates from landfills can contaminate soils, groundwater, and rivers (Viganó et al., 2015). From an economic perspective, the cost of landfilling wasted food in the US is estimated at $750 million per year and uses 4% of the total U.S. oil consumption (Gunders and Bloom, 2017). Therefore, appropriate approaches to alleviating some of these challenges are needed.

There are various valorization methods for food waste that can result in extraction of value-added compounds (polyphenols, pectin, protein), bio-materials (bio-chemicals, bio-polymers, enzymes, single cell proteins, and bio-fertilizers), compost/soil amendments, and biofuels; among the methods are biochemical conversions (anaerobic digestion and fermentation), and thermochemical conversions (pyrolysis, gasification, and hydrothermal liquefaction) (Nawaz et al., 2006; Masmoudi et al., 2008; Sowbhagya and Chitra, 2010; Hassan et al., 2013; Wang et al., 2014; Gu et al., 2019; Cheng et al., 2020a). Two major challenges for composting and other biochemical conversions are the high sensitivity of microorganisms to operating conditions and the long processing times (Pham et al., 2015). The high moisture content (60–90%) of food waste prevents thermochemical conversion technologies (pyrolysis and gasification) from achieving a net positive energy balance, whereas hydrothermal processes do not require drying the biomass and can be net energy positive.

Hydrothermal liquefaction (HTL) is a thermochemical valorization process that converts many types of biomass into an energy-dense bio-crude oil and co-products: gases, aqueous phase, and char. Among the feedstocks that have been studied are lignocellulosic biomass (Christensen et al., 2014; Zhu et al., 2014; Alhassan et al., 2016; Zhang et al., 2018; Cheng et al., 2020b), micro-and macro-algae (Zhou et al., 2010; Anastasakis and Ross, 2011; Duan and Savage, 2011; Jena et al., 2011; Vardon et al., 2011; Cheng et al., 2018), manure and animal byproducts (Chen et al., 2014; León et al., 2019), sludge from municipal wastewater treatment plants (Snowden-Swan et al., 2016; Kapusta, 2018), and food processing waste (Déniel et al., 2016; Zhang et al., 2018; Bayat et al., 2019). HTL utilizes sub-critical water (200–370°C; 10–30 MPa) to decompose complex macro-molecules into lower-molecular-weight products that then polymerize into larger compounds that form bio-crude oil. HTL bio-crude oil has lower oxygen content and higher energy density compared to products from other thermochemical conversions (pyrolysis, gasification), and can be upgraded into conventional hydrocarbon fuels or can be used directly as the source of bio-phenols and bio-polyols (Cheng et al., 2010; Li et al., 2016). HTL-char and aqueous phase can be utilized as fertilizers (Lu et al., 2018), adsorbents, and wastewater treatments (Qambrani et al., 2017). HTL yields depend on reaction temperature, residence time, heating rate, catalyst loading, and biomass composition (Anastasakis and Ross, 2015; Gollakota et al., 2018; Madsen and Glasius, 2019).

HTL of food waste has been studied by a number of researchers (Viganó et al., 2015; Motavaf and Savage, 2021). The highest bio-crude oil obtained from HTL of food residues at 300°C was 90, 75, and 10 wt.% for meats, cheeses, and fruits, respectively (Kostyukevich et al., 2018). The addition of an acid catalyst to HTL of carbohydrate-rich food waste increased bio-crude oil yield from 25 to 43 wt.% (Posmanik et al., 2017). In another study, addition of inexpensive red mud and red clay catalysts to HTL of food waste at 300°C for 1 h increased the bio-crude oil yield and promoted the thermal reaction rate; similar families of molecules in bio-crude oil with and without catalysts were observed (Cheng et al., 2020c). Model compounds have been studied to understand their effects on bio-crude oil yield and physicochemical and thermal properties (Aierzhati et al., 2019; Chen et al., 2019b). HTL temperature showed a strong effect on bio-crude oil yield and properties during HTL of fruit peel at 300–350°C and 30–120 min; the bio-crude oil yield obtained at 350°C was relatively low (Chen et al., 2020). Motavaf and Savage (2021) studied a wide range of temperatures (200–600°C) to investigate isothermal and fast HTL. The highest bio-crude oil yield from fast HTL was as high as the highest yields from isothermal HTL (28–30 wt.% at 300–400°C). Recently, a study on co-HTL of pistachio hulls and polypropylene (PP) showed that HTL can be a promising method for valorization of food waste and associated plastic materials with the addition of hydrogen donor solvents and catalysts under typical conditions (<350°C) (Hongthong et al., 2020).

A major limitation in previous studies for the characterization of bio-crude oil chemistry is the dependence on gas chromatography mass spectroscopy (GC/MS), which is not able to detect many of the compounds in bio-crude oil (Aierzhati et al., 2019; Chen et al., 2019a; Marx et al., 2020). High-resolution Fourier transform ion cyclotron resonance mass spectrometry (FT-ICR MS) has been employed to characterize highly complex samples like fossil fuels (Shi et al., 2010), algal HTL bio-crude oil (Cheng et al., 2019), pyrolysis bio-oil (Palacio Lozano et al., 2020), and natural resin (Vahur et al., 2012; Cheng et al., 2020b). FT-ICR MS provides high mass resolution and mass accuracy, and is able to resolve thousands of small mass splits in complex samples. The integration of data from different ionization techniques in FT-ICR MS enables identification of unique molecular formulae. Understanding the properties of food waste bio-crude oil will play a key role in finding industrial applications for the products, optimizing the HTL process, and improving the strategies for upgrading bio-crude oils into transportation biofuels. In this study, HTL reaction conditions were varied to identify the effects of time and temperature on the mass and energy balances for food waste conversion, extending the more typical physical and chemical characterization of bio-crude oil and HTL co-products with additional techniques to provide a more complete picture of the compounds present.

MATERIALS AND METHODS

Materials

Food waste was collected from New Mexico State University's Taos Restaurant dining hall in Las Cruces, New Mexico. Collected food waste was a mixture of meats, bread, pasta, fries, cheese, vegetables (tomato, brussel sprouts, and lettuce), fruits, and salad dressing. All packing materials, plastics, napkins, and meat bones were removed by hand. The separated organic waste fraction was mixed with deionized water using a blender to create a slurry and then frozen at −20°C prior to HTL experiments.

Hydrothermal Liquefaction of Food Waste

All HTL experiments were conducted in a stainless steel 100 ml Parr bench top reactor Model 4593. Food waste slurry (40 g at 15 wt.% solids) was mostly thawed to room temperature and transferred into the reactor. The reactor was purged with nitrogen to remove air and pressurized to ∼140 kPa with

nitrogen gas before heating to help prevent water evaporation during heating. The reactor was heated to the selected temperature (240, 265, or 295°C) by a heating jacket under constant agitation (300 rpm); once at the selected temperature, the reaction was either quenched immediately (0 min residence time) or held at the target temperature for 30 or 60 min before quenching. Once the reactor had cooled to room temperature using a fan, the gaseous products were vented. Hexane (30 ml) was added to the reactor and stirred for 3 min, then the product mixture was centrifuged (Sigma-Aldrich) at 9,000 rpm for 4 min. The solid product (HTL-char) was separated from the mixture by filtration and dried at 60°C for 48 h. Hexane-soluble bio-crude oil was separated from the aqueous phase using a separatory funnel. The hexane was removed from the bio-crude oil by rotary evaporation. HTL experiments were performed in duplicate, with measured yields agreeing to within ±3%.

Yield (wt.%) was calculated using (Equation 1):

$$\textbf{Yield (wt.\%)} = \frac{\mathbf{m_{product}}}{\mathbf{m_{feedstock,\ db}}} \times \mathbf{100\%} \quad (1)$$

where $m_{product}$ and $m_{feedstock,db}$ are the mass of products and initial feedstock on dry basis, respectively.

The recovery of carbon and nitrogen were defined as the ratios of carbon or nitrogen (wt.%) in the HTL products to the carbon or nitrogen in the original feedstock.

$$\textbf{Carbon recovery (\%)} = \frac{\mathbf{C_{product} \times m_{product}}}{\mathbf{C_{feedstock} \times m_{feedstcok,db}}} \times \mathbf{100\%} \quad (2)$$

$$\textbf{Nitrogen recovery (\%)} = \frac{\mathbf{N_{product} \times m_{product}}}{\mathbf{N_{feedstock} \times m_{feedstcok,db}}} \times \mathbf{100\%} \quad (3)$$

where $C_{product}$, $N_{product}$, $C_{feedstock}$, and $N_{feedstock}$ are the carbon and nitrogen concentration (wt.%) in the products and feedstock, respectively, on dry basis.

HTL energy recovery (ER) was calculated by Equation (4):

$$\textbf{ER (\%)} = \frac{\mathbf{HHV_{product} \times m_{product}}}{\mathbf{HHV_{feedstock} \times m_{feedstock,\ db}}} \times \mathbf{100\%} \quad (4)$$

where *HHV* is the higher heating value ($MJ \cdot kg^{-1}$) of the product or feedstock, and *m* is the weight (g) of the product or feedstock.

To compare the conversion process energy to energy recovered in bio-crude oil, an energy consumption ratio (ECR) was calculated according to Equation (5) (Vardon et al., 2012):

$$\mathbf{ECR_{HTL}} = \frac{\mathbf{[C_{PW} w_i + (1 - w_i)\, C_{Pf}]\, (T - 25)\, [1 - R_h]}}{\mathbf{Y\, (HHV)\, (1 - w_i)\, R_c}} \quad (5)$$

where w_i is the feedstock moisture content; *Y* is the bio-crude oil yield; *HHV* ($kJ \cdot kg^{-1}$) is the higher heating value of the bio-crude oil; *T* is the reaction temperature; R_h and R_c are the efficiencies of heat recovery and combustion, assumed to be 0.5 and 0.7, respectively; C_{pw} is the specific heat of water ($4.18\ kJ \cdot kg^{-1} \cdot K^{-1}$), and C_{pf} is the specific heat of the food waste ($kJ \cdot kg^{-1}\ K^{-1}$ dry basis) as per (Equation 6):

$$\mathbf{C_{pf} = 1.424 X_{carbohydrate} + 1.549 X_{protein} + 1.675 X_{lipid} + 8.37 X_{ash}} \quad (6)$$

where *X* is the mass fraction (%) of each of the component groups (Heldman, 2001).

Statistical Analysis

A full factorial experimental plan with two factors and three levels was adopted for this study. The influences of temperature and time (independent variables) on the yields of products (dependent variables) were assessed by means of an analysis of variance (ANOVA) using SPSS Statistics Data Editor (SPSS, IBM, USA) followed by least significant difference (LSD) test at a probability level ($P \leq 0.05$).

Characterization

The moisture content of the food waste was determined using a freeze dryer (Labconco, Kansas City, MO). Proximate analysis of food waste (15 ± 2 mg, dry basis) and volatilization of bio-crude oil were analyzed with a Q500 thermogravimetric analyzer (TA Instruments, New Castle, DE) using platinum pans under nitrogen and air atmospheres, respectively (ASTM E872-82). Bio-crude oil burnout temperature (T_b) and ignition temperature (T_i) were evaluated using the intersection and conversion method (Tognotti et al., 1985; Lu and Chen, 2015). The combustion characteristic index (S) of bio-crude oil was calculated as per the following (Jian-yuan and Xue-xing, 1987; Ren et al., 2014):

$$\mathbf{S} = \frac{\mathbf{DTG_{max} \times DTG_{mean}}}{\mathbf{T_i^2 \times T_b}} \quad (7)$$

where DTG_{max} and DTG_{mean} are the peak and mean of differential thermogravimetry (DTG) curves. The flammability index (Cr) of bio-crude oil was calculated following (Chen et al., 2018):

$$\mathbf{Cr} = \frac{\mathbf{DTG_{max}}}{\mathbf{T_i^2}} \quad (8)$$

The energy content (HHV) of the food waste, bio-crude oil, and HTL-char were measured using a model 6725 semi-micro bomb calorimeter (Parr Instrument Co., Moline, IL); samples were analyzed at least in duplicate. The contents of protein and carbohydrate in the food waste were measured using NREL methods (Hames et al., 2008; Sluiter et al., 2008); all measurements were done in at least duplicate. Food waste lipid content was determined according to the Folch method (Folch et al., 1957). The CHNS elemental content of the dry food waste, HTL-char, and bio-crude oil were measured using a Series II 2400 elemental analyzer (Perkin Elmer, Waltham, MA). Oxygen content was calculated by difference: O (%) =100 – [C (%) + H(%) + N(%) + S(%)]. Total carbon and total nitrogen in the aqueous phase were quantified using a model TOC-VCPH analyzer (Shimadzu Corp., Kyoto, Japan).

Fatty acid methyl esters (FAME) in the bio-crude oil were characterized using a Varian 3900 gas chromatograph (GC)

equipped with a flame ionization detector (FID). Samples were prepared by adding 200 μL of chloroform/methanol (2:1) and 300 μL of 0.6 M sulfuric acid/methanol, esterifying the samples in an oven at 80°C for 2 h, cooling the samples to room temperature, and adding 1 mL of HPLC-grade hexane. Bio-crude oil samples and feedstock for FAME analysis were further diluted to 1:9:10 and 1:1:2, respectively, with hexane and an internal standard of C23:0 methyl tricosanoate (Sigma Aldrich, St. Louis, MO), respectively. A 37-component FAME mixture (Sigma Aldrich, St. Louis, MO) was used to generate a calibration curve. Prepared samples (1 μL) were injected into a DB-23 capillary column (60 m, 0.25 mm internal diameter, 0.15 μm film thickness; Agilent Technologies, Palo Alto, CA, USA) with helium used as the carrier gas. The oven temperature was held at 50°C for 1 min, raised to 175°C at 25°C/min, and then increased at 4°C/min to 230°C.

Heteroatom-containing compounds of bio-crude oil were characterized using a custom-built 9.4 T FT-ICR mass spectrometer at the National High Magnetic Field Laboratory at Tallahassee, Florida (Kaiser et al., 2011). Food waste bio-crude oil was dissolved in 50:50 chloroform: methanol to create 1 mg/mL stock solutions. Stock solutions were then diluted to a final sample concentration of 100 μg/mL in 25:75 chloroform: methanol with either 1% formic acid, for positive-ion electrospray ionization (ESI), or 1% ammonium hydroxide solution (28% in methanol), for negative-ion ESI, to ionize basic and acidic compounds for detection by mass spectrometry. For positive-ion atmospheric pressure photoionization (APPI), stock solutions were diluted to a final concentration of 50 μg/mL with 90:10 methanol: toluene prior to analysis of polar and non-polar species. Multiple (50) individual time-domain transients were co-added, Hanning-apodized, zero-filled, and fast-Fourier-transformed prior to frequency conversion to mass-to-charge ratio (Ledford et al., 1984) to obtain the final mass spectra. Data collection was facilitated by a modular ICR data acquisition system (PREDATOR) (Blakney et al., 2011). Mass spectral lists were generated with PetroOrg software (Corilo, 2014). Internal calibration of the spectra was based on homologous series whose elemental compositions differ by integer multiples of 14.01565 Da (i.e. CH_2) (Kendrick, 1963; Savory et al., 2011). Data were visualized by relative abundance histograms for heteroatom classes with >1% relative abundance, and from isoabundance-contoured plots of double bond equivalents (DBE = number of rings + double bonds to carbon) vs. carbon number for members of a single heteroatom class. The relative abundance scale for the plots was scaled to the most abundant species in the mass spectrum.

RESULTS AND DISCUSSION

Food Waste Characterization

The proximate and ultimate compositions of the food waste are listed in **Table 1**. Lignin content is not included due to the low amount of lignin content in the sample (<0.5 wt.%). The ash content was moderately low, a positive quality for biofuel production; high ash content hinders bio-crude oil production in HTL (Chen et al., 2017b). The percentage of carbon, oxygen, and nitrogen were within the range of common blended food waste in Zhang et al. (2013). Despite variation in food waste fractions in other studies, a high degree of similarity in composition is reported for key analytical parameters, as shown in **Table 1**.

HTL Product Distribution

Figure 1A illustrates the effect of reaction temperature and time on the yield of HTL products. The maximum bio-crude oil yield (27.5 wt.%) was obtained at the lowest temperature (240°C) and 30 min reaction time. Bio-crude oil and HTL-char yields decreased with increasing temperature to 295°C for the same reaction time of 30 min, down to 15.6 and 21.7 wt.%, respectively, which was consistent with previous studies (Alhassan et al., 2016). This trend was also observed for the two other reaction times (0 and 60 min). As reaction temperature increases, molecules in bio-crude oil repolymerize or decompose into non-condensable gases, leading to increased gas yields, from 19.6 wt.% at 240°C to 44.5 wt.% at 295°C for the 0 min reaction time. HTL of high-lipid biomass generates less bio-crude oil at high temperatures because of the fast decomposition of lipids compared to the decomposition of proteins and carbohydrates (including saccharides and lignin). Feedstocks containing high amounts of crude fat and non-fibrous carbohydrates typically have the highest bio-crude yields at lower temperatures (220–275°C) and shorter reaction times (5–30 min) (Peterson et al., 2008; Pavlovic et al., 2013; Cheng et al., 2018).

HTL-char yields ranged from 21.7 to 37.8 wt.%. The highest yield was obtained at 245°C and 0 min, whereas the lowest yield was obtained at 295°C and 60 min. The decrease in HTL-char yields was attributed to the increased hydrolysis of the biomass, resulting in the formation of more bio-crude oil (Dandamudi et al., 2020). At the longer residence times, no significant reduction in HTL-char yield was observed at higher temperatures, similar to what was observed in Shakya et al. (2015). Inorganic compounds in the HTL-char cannot be converted to other HTL products, regardless of increasingly severe conditions (Watson et al., 2020).

The decrease in aqueous phase yields, and the increase in gas yields, with increasing temperature were observed because of the decomposition of some water-soluble molecules. These include cellohexaose, cellopentaose, glyceraldehydes, furfural, and protein-derived amino acids undergoing reactions such as decarboxylation, dehydration, decarbonylation, and hydrodenitrogenation to convert to less-polar compounds and more gaseous compounds like CO_2, NH_3, and CH_4 (Posmanik et al., 2017; Watson et al., 2020).

The influence of increasing reaction time on bio-crude oil yield is highly dependent on reaction temperature. At 240°C, bio-crude oil yield increased from 23.1 wt.% at 0 min to 27.5 wt.% at 30 min but decreased at 60 min to 18.8 wt.%. At 295°C, bio-crude oil yield decreased continually with longer reaction time. Aierzhati et al. (2019) reported that bio-crude oil yield from food waste increased with reaction times from 0 to 40 min, but plateaued beyond 60 min. In another study, bio-crude oil yield decreased from 20 to 15% when the reaction time was increased from 15 to 30 min (Anastasakis and Ross, 2011). These results suggest that the feedstock is converted into bio-crude

TABLE 1 | Biochemical and elemental composition of food waste feedstock as the mean of at least duplicate analysis.

		This study (wt.%)	(Cheng et al., 2020c)	(Aierzhati et al., 2019)	(Motavaf and Savage, 2021)	(Chen et al., 2019a)
Proximate analysis (wt.%)[a]	Moisture content[b]	72.7 ± 0.5	73.0	70.1 ± 0.1	–	74.0
	Ash	3.3 ± 0.3	1.1	4.7 ± 0.1	5.4	1.1
	Volatile matter	83.7 ± 0.2	–	–	–	24.8[f]
	Fixed carbon	12.9 ± 0.2	–	–	–	
Biochemical analysis (wt.%)[a]	Carbohydrate	52.8 ± 0.4	58.9	77.0	51.4	52.5
	Lipid	20.5 ± 0.6	21.9	36.5	15.7	2.0
	Protein	21.4 ± 0.1	17.8	24.0	27.5	26.4
Elemental analysis (wt.%)[a]	Carbon	48.9 ± 1.2	44.5[d]	56.2 ± 1.2	47.8	51.3
	Hydrogen	6.2 ± 0.2	6.4[d]	8.0 ± 0.1	5.1	7.6
	Nitrogen	3.4 ± 0.5	3.8[d]	2.6 ± 0.2	4.8	4.4
	Sulfur	1.5 ± 0.2	–	–	0.2	0.4
	Oxygen[c]	39.7 ± 1.6	45.4[d]	33.2 ± 0.9	42.1	36.2
	HHV (MJ/kg)	20.9 ± 0.7	24.6[e]	24.5 ± 0.3	22.3	22.7

± = standard deviation.
[a]Dry basis; [b]As received basis; [c]By difference; [d]Standard deviation is < ±1.2 wt.%; [e]Standard deviation is < ±1 MJ kg^{-1}; [f]Sum of volatile matter and fixed carbon.

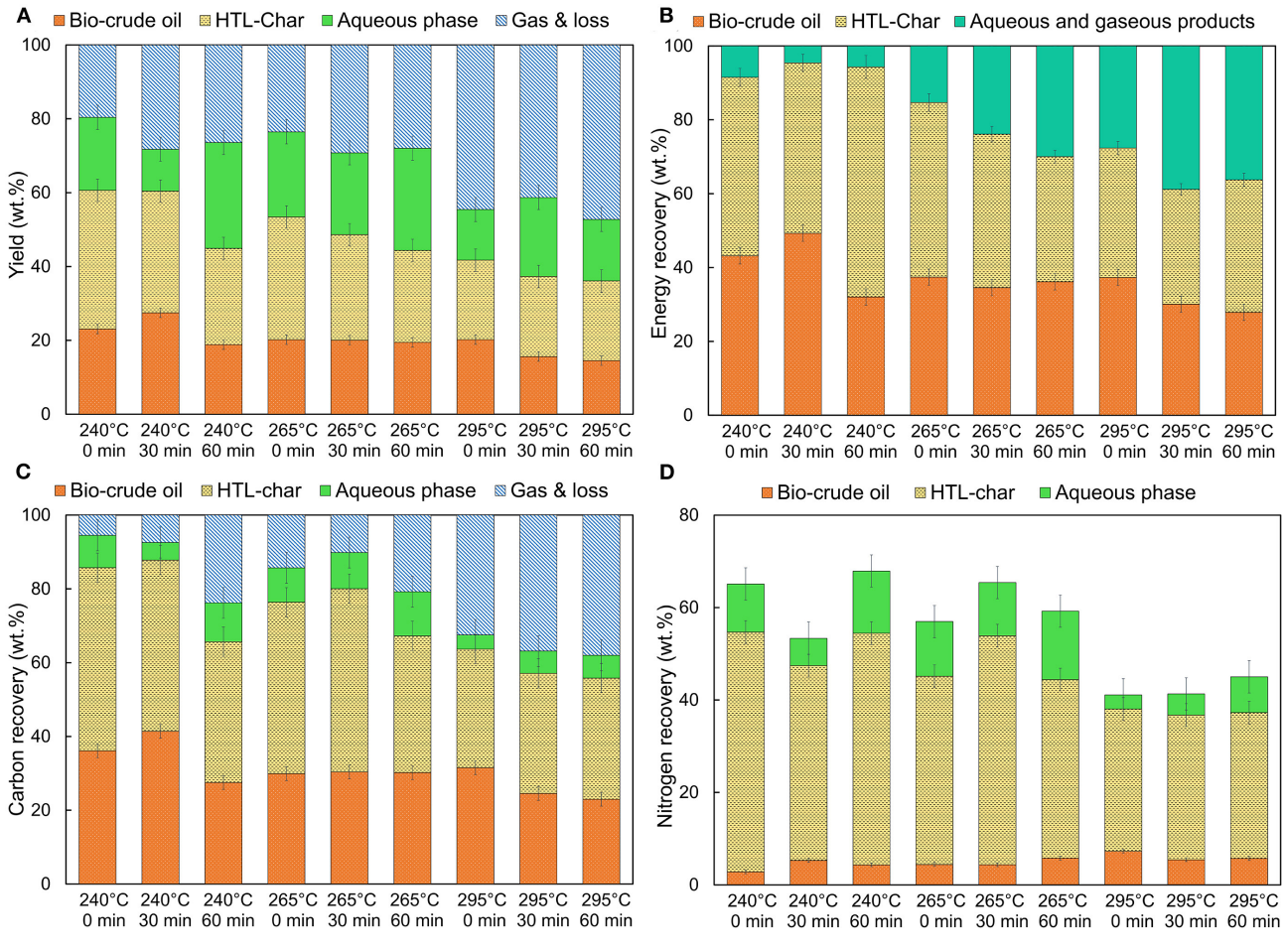

FIGURE 1 | Distribution of **(A)** mass, **(B)** energy, **(C)** carbon, and **(D)** nitrogen in wt.% dry weight basis across range of different operating conditions for HTL of food waste. Standard deviation is < ±1.5 wt.% for **(A–C)** and < ± 0.5 wt.% for **(D)** for duplicate experiments.

oil and HTL-char first, then bio-crude oil and aqueous phase components are converted into gaseous products.

Energy Recovery and Energy Consumption Ratio

The influence of temperature and reaction time on the ER for bio-crude oil and HTL-char from food waste are shown in **Figure 1B**. The highest HHV of bio-crude oil (40.2 MJ/kg) was obtained at 295°C and 30 min (**Supplementary Table 1**) as carbohydrate and protein compounds were converted to produce bio-crude oil (Cheng et al., 2018), which is in line with the HHV of bio-crude oils derived from food waste in previous studies (32–41 MJ/kg) (Zastrow and Jennings, 2013; Maag et al., 2018; Zhang et al., 2018). The highest energy recovery for food waste bio-crude oil (49.3%) was comparable to recovered energy from HTL of algae (Gai et al., 2014) and other lignocellulose biomass (Cao et al., 2017). Reaction time only appeared to have a noticeable effect on energy recovery at 295°C, where an increase from 0 to 60 min lead to a decrease from 37.3% to 27.9 wt.%. At low temperatures and short reaction times, the majority of the biomass energy remains within the HTL-chars. Increasing temperature leads to more organic components from the feedstock partitioning into the aqueous phase and gaseous products, reducing the energy recovery for bio-crude oil. Here, the energy recovery of aqueous phase and gaseous products together increased from 8.5 to 38.82 wt.%. Despite the higher gas yield at 295°C, Brown et al. (2010) showed that gaseous products from HTL of microalgae have a low HHV under subcritical water conditions (<375°C); gas products obtained at 200°C contained 88.0% CO_2 and 0.39% H_2 with a HHV of 0.03 MJ/kg, compared to gas products obtained at 300°C, which contained 91.5% CO_2 and 5.1% H_2 with a HHV of 4.2 MJ/kg. The gas becomes richer in hydrocarbons (CH_4 and C_2 compounds) as the hydrothermal processing temperature increased from 350 to 500°C, leading to higher energy recovery.

The value of the energy consumption ratio (ECR) for bio-crude oil from food waste shows that HTL at low temperature is energy-positive (ECR = 0.6) (**Supplementary Table 1**). Increases in temperature and reaction time caused to ECR to be greater than unity, which means that HTL at more severe conditions is not a net energy producer. Higher ECR is directly related to lower bio-crude oil yield and lower energy content of products (Equation 5). Increasing temperature leads to increasing the amount of heat needed to warm the water, which is reflected in the ECR results. Anastasakis and Ross (2015) reported that ECR increased with an increase in temperature.

Carbon and Nitrogen Recovery Within HTL Products

Figure 1C shows the carbon recovered in the HTL products relative to the carbon in the food waste feedstock. Carbon recovery in bio-crude oil and HTL-char ranged from 23.0 to 41.4 wt.% and 32.2 to 49.7 wt.%, respectively, which are consistent with the results from HTL of high-carbohydrate biomass. Li et al. (2013) showed that much of the carbon is transferred into the char phase, with smaller fractions into the liquid (10–40%) and gas phases (<10%) at moderate HTL temperatures (160–300°C) for high-cellulosic content feedstocks. Carbon recovery for bio-crude oil decreased dramatically from 41.4 to 24.5 wt.% with increasing reaction temperature from 240 to 295°C for 30 min. The highest temperature leads to release of a significant portion of carbon into the gaseous phase. Carbon recovery within the bio-crude oil was highest at 30 min for lower temperatures; for higher temperatures, carbon recovery decreased with increasing reaction time. Increasing the reaction time led to a similar decrease in HTL-char carbon recovery, except at 295°C when the carbon recovery appeared to plateau. It is noteworthy that the carbon content of bio-crude oil did not change substantially with reaction conditions (**Supplementary Table 1**), therefore, the changes in carbon recovery in bio-crude oil are primarily associated with bio-crude oil yield, as was reported in previous studies (Gai et al., 2014; Zhu et al., 2017).

Carbon recovery in the aqueous phase decreased with increasing temperatures to 6.0 wt.%. Xu et al. (2018) also reported that carbon recovery within the aqueous phase from HTL of sewage sludge reduced with increasing temperature from 260 to 350°C. This is caused by the abundance of certain organic and alcohol compounds in the aqueous phase at low temperatures (Lu et al., 2017). Tian et al. (2015), however, found that carbon partitioning to the aqueous phase increased slightly with increasing temperature.

The presence of N-containing compounds is a major challenge for the utilization of bio-crude oil as fuel. Understanding the fractionation of N, therefore, is needed for optimization of HTL. Here, nitrogen recovery in the bio-crude oil increased from 2.8 to 7.3 wt.% with increasing reaction temperature, in agreement with previous studies (Gai et al., 2014; Tekin et al., 2016; Tang et al., 2019). Proteins can decompose at high temperatures *via* Maillard, amidation, esterification, and rearrangement reactions between lipids and proteins, or between proteins and reducing sugars (Biller and Ross, 2011; Vardon et al., 2011; Leow et al., 2015).

The highest nitrogen recovery was obtained in HTL-char for low temperatures and short reaction times (**Figure 1D**). Typically, the presence of glucose in lignocellulosic biomass inhibits nitrogen transfer to the bio-crude oil and aqueous phases (Qiu et al., 2019). Char with high nitrogen content used as an organic fertilizer can increase the amount of available nitrogen and phosphorous, increase crop yields, and reduce greenhouse gas emissions (Al-Wabel et al., 2018; Islam et al., 2021). Adjuik et al. (2020) showed that CO_2 fluxes were 34% lower in HTL-char treated soils than in the control treatment. In order to increase the economic viability of bio-crude oil production from food waste, the value-added application of food waste HTL-char could be considered for future studies. Due to its high oxygen content (**Supplementary Table 1**), the HTL-char obtained in this study has been identified as a desirable adsorbent for heavy metals removal from wastewater (Bayat et al., 2020).

The aqueous phase from HTL of food waste showed a low nitrogen recovery, ranging from 4.5 to 14.8 wt.% (TN = 0.74–1.8 g/L), in agreement with previous studies (Gu et al., 2019). Watson et al. (2020) reported that the aqueous phase derived from HTL of lignocellulosic biomass, or a feedstock dominated by carbohydrates, has the lowest nitrogen content ($TN_{average}$ = 0.8 g/l) compared to the aqueous phase from HTL of manure,

algae, or sludge due to the low amounts of protein-containing compounds. No clear trends were observed between nitrogen recovery in the aqueous phase and the operating conditions tested here.

TGA of Bio-Crude Oil

As shown in **Figure 2A**, heating bio-crude oil to 800°C in an air atmosphere resulted in a total weight loss of 93–98%. Three weight loss peaks were observed in all bio-crude oil samples during combustion (**Figure 2B**), resembling the results in Chen X. et al. (2020). The main weight loss was observed in the first stage between 50 and 320°C due to volatilization and oxidation of light compounds. The second stage, from 320 to 480°C, is designated as the fuel deposition stage (Yuan et al., 2018), indicating decomposition and isomerization reactions. As the temperature further increased above 500°C, the formation and combustion of coke occurred. Bio-crude oil obtained at 290°C and 60 min had the highest weight loss rate, implying that higher temperature HTL favored the production of more volatile compounds. The ignition characteristics of the bio-crude oil (ignition temperature, burnout temperature, and combustibility characteristics index) evaluated by DTG are listed in **Table 2**. Bio-crude oil ignition temperature (T_i) increased slightly from 220 to 255°C as the HTL reaction temperature increased from 240 to 295°C. This indicates that the bio-crude oil obtained at low temperature contained lower-molecular-weight compounds that need less energy for decomposition, resulting in lower ignition temperatures. The difficulty for ignition of bio-crude oil is likely due to the low content of hydrocarbons in the bio-crude oil. The ignition temperature of bio-crude samples is similar to crude oil (>204°C) and jet fuels (210°C), and lower than heavy fuel oil, castor oil, and sludge pyrolytic oil (EngineeringToolBox, 2003; Chen et al., 2017a). Lower burnout temperatures (T_b) were observed for the bio-crude oils produced at higher temperatures. As shown in **Table 2**, the S and Cr value for the bio-crude oils had a similar trend to ignition temperature, where the highest S value of 14.48 and Cr of 3.1 were observed for bio-crude oil created at 295°C, indicating the combustion properties were improved by increasing the HTL temperature, in agreement with Chen et al. (2019a). They compared the combustion properties of bio-crude oil from food waste HTL at 320°C and 30 min with the combustion properties of bio-crude oil derived from swine manure and manure/crude glycerol reported in Wang et al. (2016). Food waste bio-crude oil gave a much higher S value (20.04) than those from swine manure (1.28) and manure/crude glycerol (0.54). In general, a higher S value indicates better combustion properties because easier ignition, shorter burnout time, and strong reaction strength (Niu et al., 2011). These combustion characteristics are important factors for evaluating fire hazards associated with the future use, storage, and shipment of bio-crude oil.

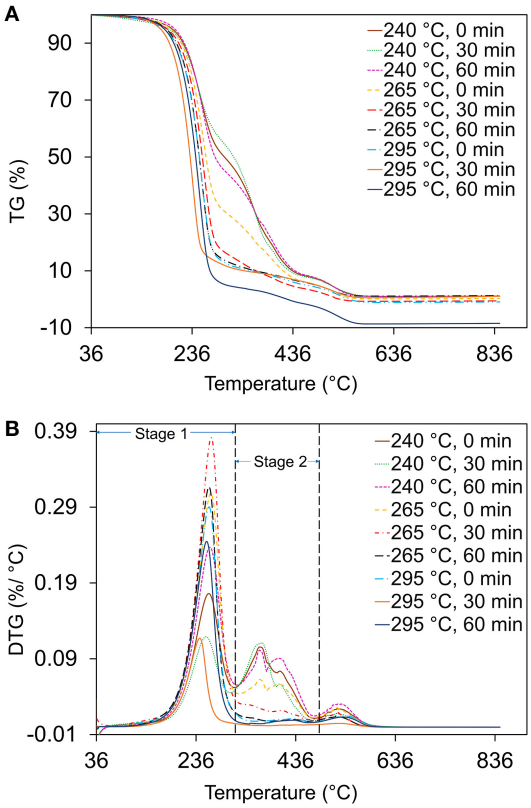

FIGURE 2 | (A) Thermogravimetric analysis (weight loss) and **(B)** differential thermogravimetric analysis (weight loss rate) of bio-crude oils derived from hydrothermal liquefaction of food waste under different temperature and reaction time conditions. Analysis was conducted under an air atmosphere.

FAME Analysis of Bio-Crude Oil

FAME within bio-crude oil are produced from the hydrolysis of triacylglycerides (TAGs) by sub-critical water. The distributions of FAME in bio-crude oil made under different HTL conditions are shown in **Figure 3**. A maximum of 37.1 wt.% FAME was observed in the bio-crude oil from HTL at 240°C. Total FAME content declined from 37.1 to 19.9 wt.% with increasing temperature and reaction time. This decrease correlates with the increase of other biochemical compounds (carbohydrate- and protein-derived) in the bio-crude oil, and the corresponding decrease in lipid-derived compounds with higher reaction temperature and time (Obeid et al., 2020). The presence of polyunsaturated fatty acids (C18:3N3 and C18:3N6) in bio-crude oil shows that HTL does not fully destroy unsaturated fatty acids (Palardy et al., 2017). The portion of polyunsaturated FAME (PUFAs) significantly decreased, while the saturated and monounsaturated FAME (MUAFs) slightly increased, with increased temperature and time. This means that bio-crude oil produced from food waste conserved PUAFs at lower HTL temperatures, while saturated FAMEs are more stable. Long chain fatty acids (C_{16}-C_{18}) are produced at lower temperatures, then converted to long-chain hydrocarbons at higher temperatures (Gai et al., 2015). The most abundant FAMEs in bio-crude oil were octadecatrienoic acid (C18:3N6) and trans-9 elaidic acid (C18:1T). The presence of unsaturated fatty acids, especially the polyunsaturated ones, can negatively influence the oxidation stability of bio-crude oil. Oxidation

TABLE 2 | Combustion characteristics of bio-crude oils calculated from thermogravimetric data under an air atmosphere.

HTL temperature (°C)	HTL residence time (min)	T_i (°C)[a]	T_b (°C)[b]	S × 10^{-7} (%^{2} °C^{-3} min^{-2})[c]	Cr × 10^{-4} (% min^{-1} °C^{-2})[d]
240	0	217.4	589.3	3.1	1.0
240	30	222.3	599.7	3.4	1.2
240	60	246.9	606.9	3.7	1.3
265	0	249.4	575.9	6.1	1.8
265	30	250.3	529.2	8.3	2.3
265	60	246.6	600.9	7.0	2.5
295	0	255.1	546.1	7.8	2.3
295	30	235.2	548.9	10.1	3.1
295	60	255.1	424.6	14.5	2.5

[a]*Ti, ignition temperature;* [b]T_b, *burnout temperature;* [c]*S, combustion index;* [d]*C, flammability index.*

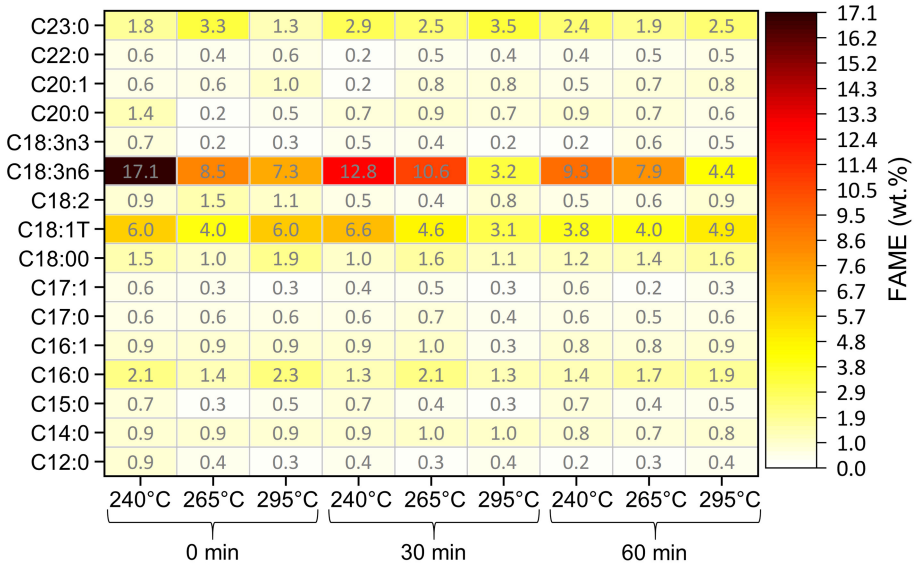

FIGURE 3 | Heat map quantifying fatty acid methyl ester (FAME) distribution in bio-crude oil under different HTL temperature and reaction time conditions. Numbers in heat map represent FAME wt.% on a dry feed basis.

increases bio-crude oil viscosity and acid value, reducing HHV and requiring further upgrading.

FT-ICR MS Characterization of Bio-Crude Oil

In order to study the effect of HTL temperature and residence time on the distribution of heteroatom-containing compounds in bio-crude oil, bio-crude oils from five different operating conditions were selected for FT-ICR MS characterization: 240°C for 0, 30, and 60 min, 265°C for 30 min, and 295°C for 30 min.

Heteroatom Class Distribution

Figure 4 shows the distribution of the most abundant heteroatom classes in the bio-crude oils derived from positive-ion APPI. The heteroatom class distribution derived from positive-ion ESI have similar trends as seen in the positive-ion APPI. The main differences were the higher relative abundance of hydrocarbon (HC) and O_x-containing compounds in positive-ion APPI due to the increased ionization efficiency of aromatic compounds. Sodiated heteroatom classes appear to be more effectively resolved with positive-ion ESI.

O_x Classes

O_{1-6} containing compounds accounted for 55–70% of the total identified heteroatom classes in all the bio-crude oil samples. The O_2 class was the most prominent class in bio-crude oils from HTL at 265 and 295°C for 30 min, while the O_4 class was the most prominent class in all samples obtained at 240°C. Deoxygenation reactions at higher temperatures convert high O-containing compounds to a more hydrocarbon-dominant products. As shown in **Figure 4A**, with increasing HTL temperature, the abundance of O_{1-2} containing compounds increased for all bio-crude oil samples, whereas that of O_{3-6} compounds decreased. This indicates the tendency for hydrogenation of

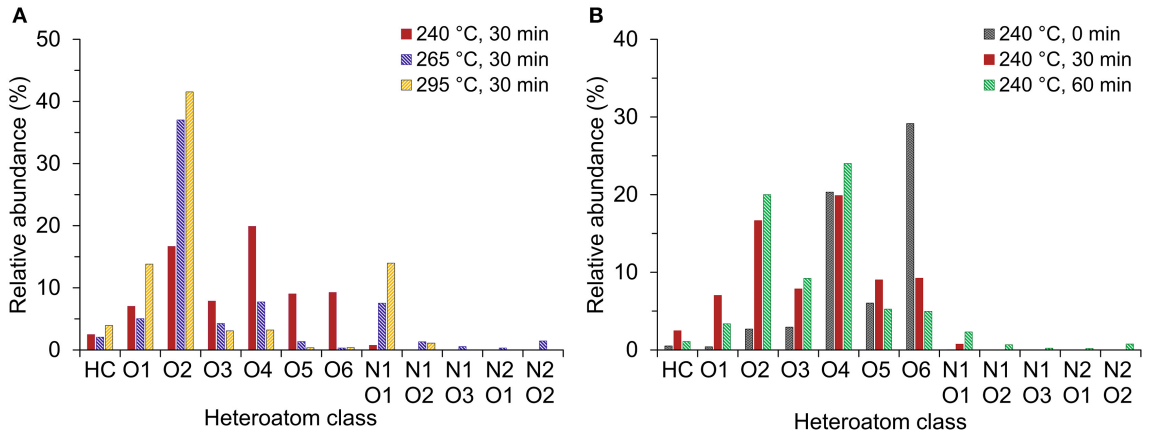

FIGURE 4 | (A) Effect of HTL temperature and **(B)** HTL reaction time on heteroatom class distribution of bio-crude oil from HTL of food waste derived from positive-ion atmospheric pressure photoionization (APPI) Fourier transform ion cyclotron resonance mass spectroscopy (FT-ICR MS).

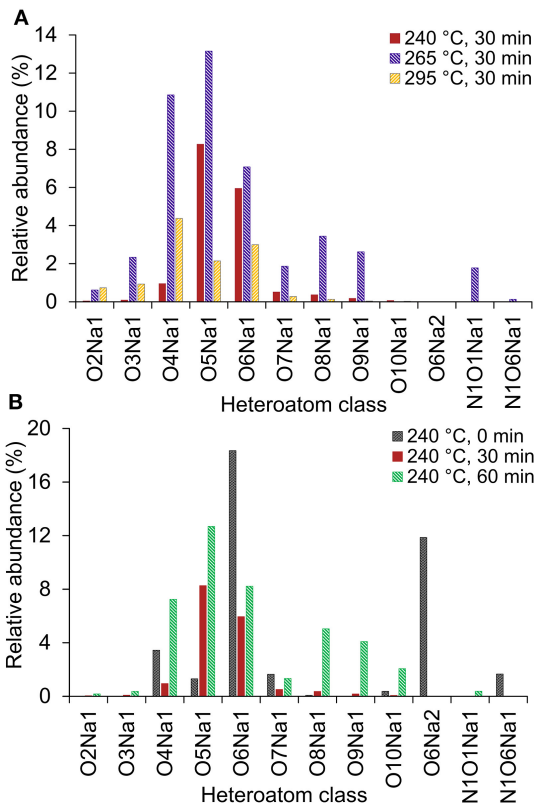

FIGURE 5 | (A) Effect of HTL temperature and **(B)** reaction time on Na-containing heteroatom class distribution on bio-crude oil from HTL of food waste derived from positive-ion Electrospray ionization (ESI) Fourier transform ion cyclotron resonance mass spectroscopy (FT-ICR MS).

unsaturated fatty acids to saturated fatty acids with increasing the temperature to 295°C, as supported by the decrease of polyunsaturated FAMEs in bio-crude oil found by FAME analysis. The O_6 class for the least severe conditions (240°C, 0 min) represented ∼30% of the bio-crude oil compounds detected—one of the most abundant classes among all samples; at 265 and 295°C, the O_6 class represented <1% of the bio-crude oil compounds. This class consists primarily of sugar derivatives, indicating the further conversion and rearrangement of sugars in higher temperatures. Promdej and Matsumura (2011) reported that sugars decomposition is accelerated with increasing temperatures, with near complete decomposition at 300°C within 60 s.

$N_{1-2}O_{1-3}$ Classes

Due to the low protein content in the feedstock (**Table 1**), a very low abundance of $N_{1,2}O_x$ (x = 1, 2, and 3) species (like pyrrole carboxylic acid, fatty acid amides B, and C) was expected in FT-ICR MS of the bio-crude oils. Abundance of N_1O_1-containing compounds increased with increasing temperature and time, with temperature having the more noticeable effect (**Figure 4**). The increase in N+O-containing compounds may be attributed to increases in Millard reactions between amino acids and sugars at high temperatures, consistent with Wu et al. (2020).

$O_{1-10}Na$ Classes

All HTL bio-crude oil samples contained a diverse range of O_{1-10}Na-containing compounds, as shown in **Figure 5**. The most abundant sodiated heteroatom class were O_4Na and O_5Na. The presence of such compounds, which were reported in previous studies (Cheng et al., 2017; Jarvis et al., 2017), may be attributed to the salt content of the collected food waste, or to glass container pieces being incorporated during food waste processing. In **Figure 5**, sodiated heteroatom classes (except O_5Na) in bio-crude oil at 240°C for 30 min represented the lowest abundance among the other four samples. For the given residence time, bio-crude oil obtained at 265°C showed the highest abundance in all individual heteroatoms of O_{1-6}Na compared to both lower (240°C) and higher (295°C) temperatures (**Figure 5A**). This shows that, with increasing

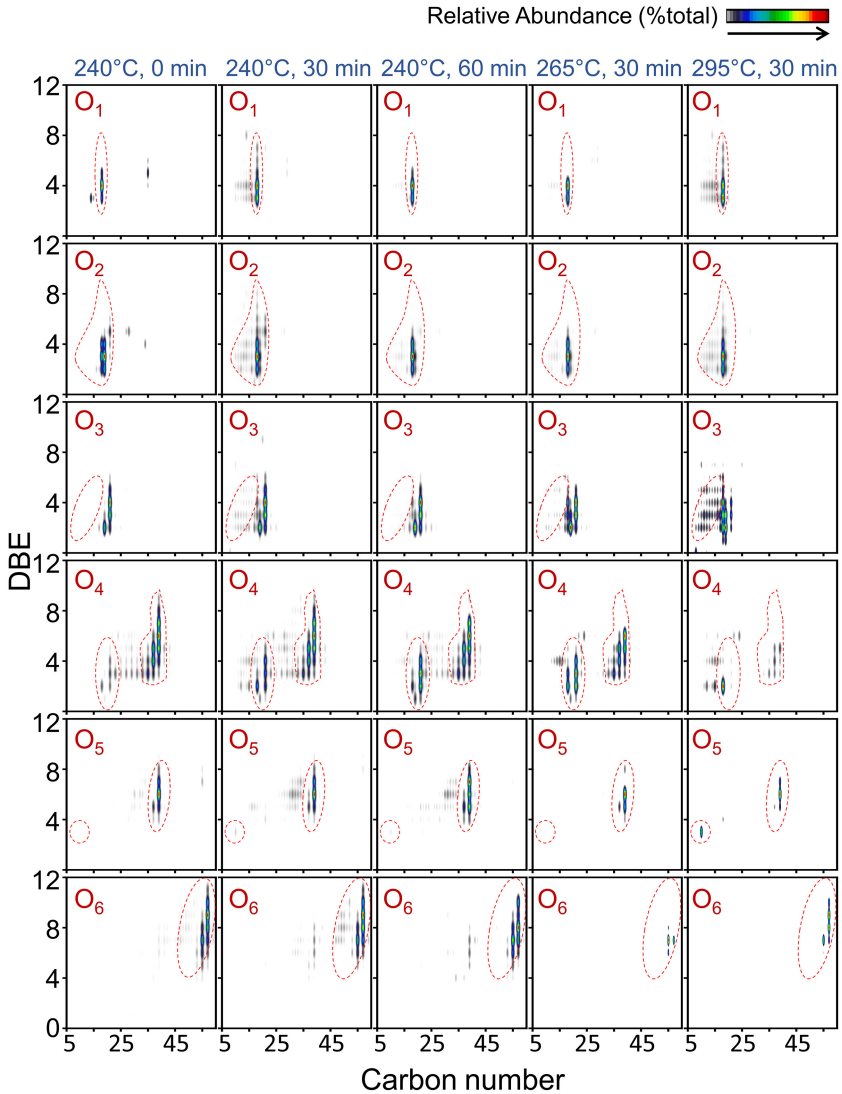

FIGURE 6 | Color-coded isoabundance contour plots for the O-containing heteroatom classes of compounds in bio-crude oil obtained at different HTL temperature and reaction time conditions observed by positive-ion APPI FT-ICR MS.

temperature, sodiated compounds tend to move to the bio-crude oil phase, then move further to the aqueous and HTL-char phases. The presence of these Na-containing classes is quite interesting as they impact fuel quality and upgrading.

HC Classes

The two most abundant hydrocarbon (HC) classes were observed in bio-crude oils from both the lowest and highest temperatures (240 and 295°C) for 30 min, suggesting that production of HC classes requires a trade-off between HTL temperature and reaction time.

Compositional Space Coverage

Differences in observed compositional space between bio-crude oils obtained at different HTL operating conditions are visualized using isoabundance-contoured plots of double bond equivalent (DBE, where DBE = # of carbon rings + double bonds to carbon) vs. carbon number for the most abundant heteroatom classes observed by positive-ion APPI and positive-ion ESI FT-ICR MS in **Figures 6**, **7**.

All bio-crude oil samples had a broad distribution of O_{1-6}-containing species over C_9-C_{59} and DBE values of 1–12 (**Figure 6**). For all bio-crude oil samples, the compositional space of O_{1-3} species (C_9-C_{34} and DBE of 1–10) covered a smaller area than O_{4-6} species (C_9-C_{62}, DBE of 1–12). All samples showed a similar pattern for the most dominant compounds: $C_{18}H_{28,30,32}O_1$, DBE of 3–5 within the O_1 class, which are most likely aromatics (e.g., phenols, alcohols and methoxyphenols and furans) derived from the glucose degradation. Glucose decomposes into unstable low-molecular-weight aldehyde and ketone fragments under HTL conditions, which then form aromatic compounds *via* condensation and

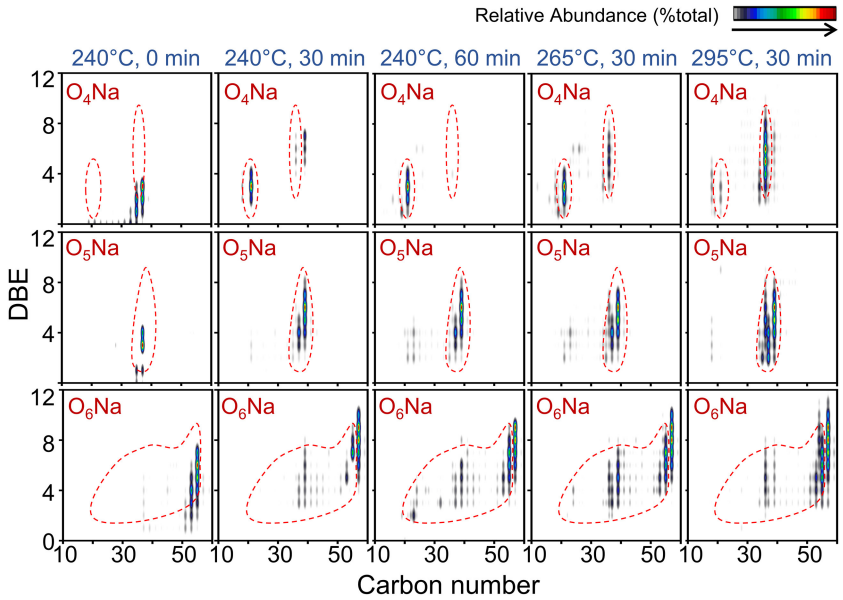

FIGURE 7 | Color-coded isoabundance contour plots for Na-containing heteroatom classes of compounds in bio-crude oil obtained at different HTL temperature and reaction time conditions observed by positive-ion ESI FT-ICR MS.

cyclization (Matayeva et al., 2019). Stanford et al. (2006) reported phenols in bio-crude oil with DBE ≥ 4 among aromatic mono-oxygen species.

Despite the variation in compositional space with HTL temperature and time, the most dominant compound classes were similar for all bio-crude oil samples. For example, while the abundance of the O_6 class varied between bio-crude oils obtained at the most and least severe conditions (295°C for 30 min and 240°C for 0 min), the most dominant compounds remained within C_{55}-C_{57} and H_{96}-H_{102}. The most abundant species from the O_2 and O_3 classes in all operating conditions had DBE values of 2–4, most likely corresponding to lipid-derived fatty acids (O_2 class) and hydroxy- and epoxy-fatty acids (O_3 class). O_2 classes with higher DBE values (>5) were identified as aromatic carboxylic acids or polycyclic naphthenic acids (Sudasinghe et al., 2014). The most abundant compounds for the O_4 class in bio-crude oil from 295°C had a wider compositional space (C_{15}-C_{39} and DBE of 2–5) than in bio-crude oil from 265°C (C_{21}-C_{39}, and DBE of 2–6) and in bio-crude oil from 240°C (C_{37}-C_{39} and DBE of 5–7). This may indicate bio-crude oil undergoes decomposition and repolymerization to non-aromatic short-chain compounds (DBE < 4) at the higher temperatures. The presence of O_x groups leads to high viscosity and strong tendency to re-polymerize, requiring further upgrading like hydrodeoxygenation techniques.

Food waste-derived bio-crude oils did not show significant contribution from N_xO_x-containing compounds. The compositional space coverage of the N_1O_1 species from positive-ion APPI FT-ICR MS is shown in **Supplementary Figure 1**. There are two distinct aromaticity ranges: non-aromatic species (DBE < 4) and aromatic species (DBE ≥ 4). The three most abundant species within all five bio-crude samples had DBE values of 2–4. The N_1O_1 species within the bio-crude oil from 240°C for 30 and for 60 min were spread over a range of C_{16}-C_{23} and DBE values of 1–5, and C_{10}-C_{26} and DBE 1–9, respectively. The N_1O_1 species within the samples from higher reaction temperatures, 265 and 295°C, ranged from C_{10}-C_{29} and DBE of 1–11, which attributed due to a higher degree of alkylation. Within the N_1O_1 class, the majority of the abundant species for bio-crude oils from higher reaction temperatures had DBE values < 4, which represents the decomposition of the aromatic structures, such as pyrrole, hydroxyl, and carbonyl, to non-aromatic amide structures (e.g., $C_{18}H_{33}N_1O_1$ and $C_{16}H_{33}N_1O_1$). The compositional space for N_1O_1 species increased with increasing reaction severity (**Supplementary Figure 1**), with increasing temperature having the greater effect on the number of identified N_1O_1-containing compounds: 20 species at 240°C vs. 114 species at 295°C, compared to 3 species at 0 min vs. 55 species at 60 min. Within the N_1O_1 class, the assigned chemical formulae of $C_{18}H_{33}NO$ and $C_{18}H_{35}NO$ were the most abundant in all bio-crude oil samples, representing fatty acid amides formed by reactions of fatty acids and protein-derived compounds (Simoneit et al., 2003) or decarboxylated amino acids from protein decomposition (Leonardis et al., 2013).

The number of rings or double bonds for O_xNa-containing compounds for all bio-crude oils ranged mostly between 1 and 11 (**Figure 7**). The two most dominant species, O_5Na and O_6Na, remained unchanged across reaction conditions: $C_{39}H_{68,70,72}O_5Na$ and $C_{57}H_{98,100,102}$ with DBE values of 5–7 and 7–9, respectively. These sodiated O-containing species are likely to be unsaturated fatty acids. The O_4Na species appeared to be more influenced by increasing the temperature from 265 to

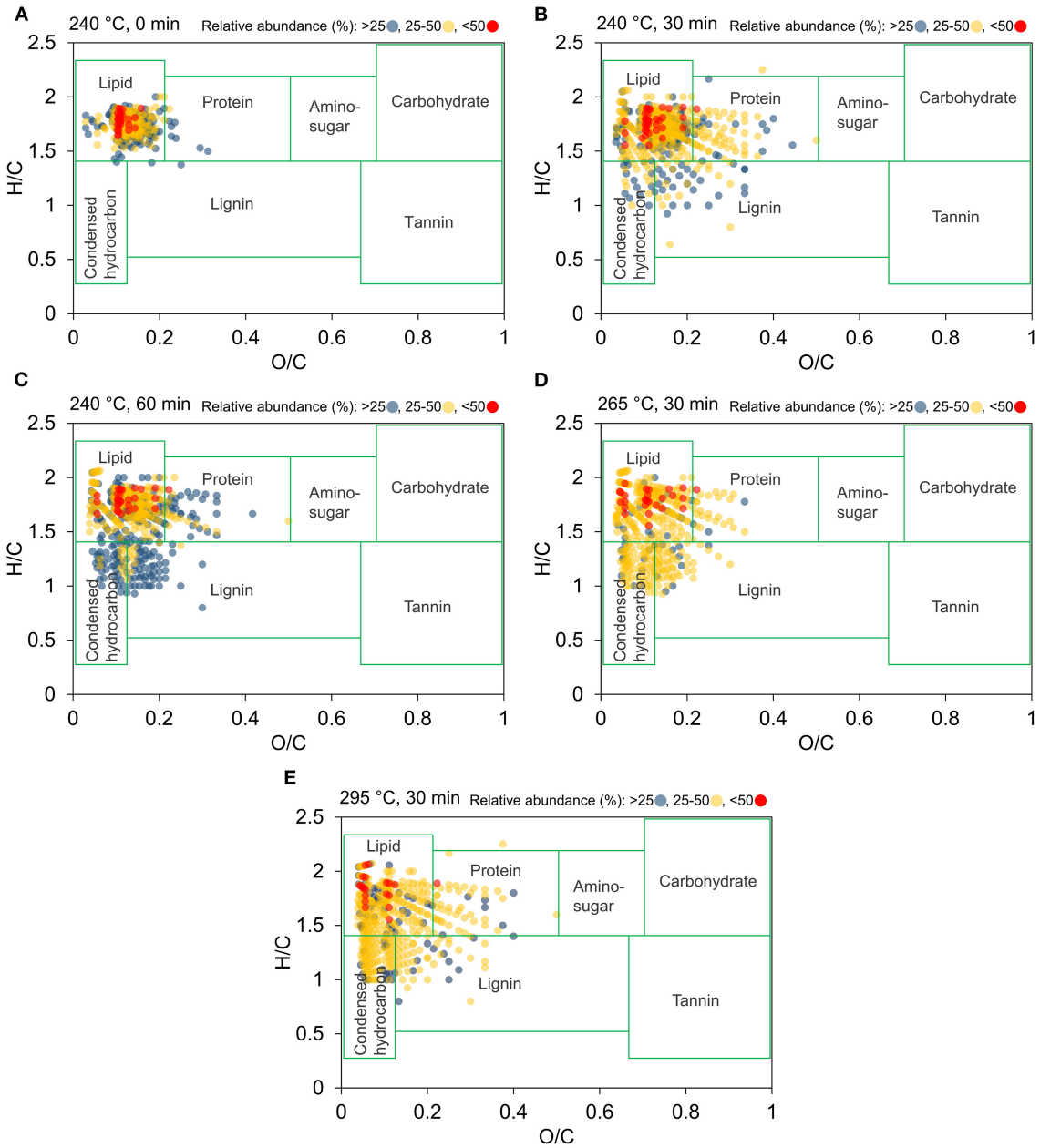

FIGURE 8 | Van Krevelen diagrams for bio-crude oil obtained from **(A)** 240°C, 0 min, **(B)** 240°C, 30 min, **(C)** 240°C, 60 min, **(D)** 265°C, 30 min, and **(E)** 295°C, 30 min based on data derived from positive-ions APPI FT-ICR MS. The relative abundance is represented by blue circles (<25%), yellow circles (25–50%), and red circles (>50%).

295°C: carbon number increased from 21 to 36 and showed a high affinity toward unsaturation, confirmed by the higher DBE average of 6 in **Figure 7**.

The compositional space for HC compounds derived from positive-ions APPI FT-ICR MS in all bio-crude samples ranged from C_{11}-C_{31} and DBE of 3–10, which are dominated by a moderate degree of aromaticity with DBE values of 5 and 6 (**Supplementary Figure 1**). $C_{18}H_{28}$, $C_{18}H_{30}$, and $C_{29}H_{48}$ were dominant in all bio-crude oil samples, representing polycyclic aromatic hydrocarbons (PAHs) and alkylated derivatives. The presence of compounds with DBE values of 9 and 10 in bio-crude oils from more severe HTL conditions indicates that polymerization and condensation reactions are more prevalent.

Van Krevelen Diagrams

In an attempt to simplify the complex data set obtained from FT-ICR MS, the molecular compositions of bio-crude oil samples were visualized in **Figure 8** as van Krevelen diagrams

using the H/C and O/C ratios (Kim et al., 2003), and relative abundance ranges. Each region of the van Krevelen diagram was assigned to a specific class of compounds, such as lipid-, lignin-, and condensed aromatic-derived. The composition type found in bio-crude oil with highest relative abundance was lipid-derived compounds, followed by protein- and condensed aromatic-derived compounds. With the increase of reaction temperature to 295°C, less oxygenated (O/C $<$ 0.3) and more saturated (H/C $>$ 1.5) compounds were observed, indicating that dehydration and deoxygenation reactions occurred. More compounds with medium relative abundances in the condensed hydrocarbon region were found when temperature increased. With respect to HTL reaction time, compounds with medium relative abundances first appear in the protein-derived and lignin-derived regions, then shift to lower O/C ratio and higher H/C regions, which correspond to lipid-derived compounds. The observed changes in elemental ratios indicate that bio-crude oils become more saturated with increasing temperature, which is consistent with the decrease of DBE in bio-crude oil obtained at more severe conditions.

CONCLUSION

Physicochemical and thermal characteristics of bio-crude oils indicate that HTL temperature and time affect HTL product outcomes for processing food waste. The highest yield (27.5 wt.%), carbon recovery (41.4 wt.%) and energy recovery (49%) for bio-crude oil are obtained at 240°C and 30 min. Increasing temperatures resulted in lower bio-crude oil yields, with more polycyclic, O-, and N-heteroatom-containing aromatic compounds, and higher bio-crude oil ignition temperatures, but also a higher combustibility index. Given these encouraging results, HTL can be a promising pathway to valorize these waste streams. FT-ICR MS analysis revealed a diverse range of bio-crude oil components. O_{2-4}, N_1O_1, and $O_{4-6}Na$ represented the most abundant species in bio-crude oil across different HTL operating conditions. Detailed chemical characterization of HTL bio-crude oil, which can help in understanding of the reactions involved in HTL process, is essential for feedstock selection and process optimization to pave the way for better applications of bio-crude oil and for further processing into new and higher-quality products.

DATA AVAILABILITY STATEMENT

The original contributions presented in the study are included in the article/**Supplementary Materials**, further inquiries can be directed to the corresponding author.

AUTHOR CONTRIBUTIONS

HB: methodology, analysis, data validation, and writing—original draft. MD: analysis and writing—review and editing. JJ: data curation and writing—review and editing. CB: supervision and writing—review and editing. UJ: supervision, conceptualization, and writing—review and editing. All authors contributed to the article and approved the submitted version.

FUNDING

The project was partially supported by the NMSU's College of Engineering faculty start-up funds.

ACKNOWLEDGMENTS

The authors acknowledge John Rivers of Sodexo for his assistance in acquiring food waste from NMSU dining Hall. A portion of this work was performed at the National High Magnetic Field Laboratory, which is supported by NSF Cooperative Agreement #DMR-1644779, the State of Florida, and the U.S. Department of Energy. The authors also acknowledge assistance from members of the Brewer Research Group, Barry Dungan, Alan Moya, and Mark Chidester at NMSU.

SUPPLEMENTARY MATERIAL

The Supplementary Material for this article can be found online at: https://www.frontiersin.org/articles/10.3389/fsufs.2021.658592/full#supplementary-material

REFERENCES

Adjuik, T., Rodjom, A. M., Miller, K. E., Reza, M. T. M., and Davis, S. C. (2020). Application of hydrochar, digestate, and synthetic fertilizer to a miscanthus X giganteus crop: implications for biomass and greenhouse gas emissions. *Appl. Sci.* 10:8953. doi: 10.3390/app10248953

Aierzhati, A., Stablein, M. J., Wu, N. E., Kuo, C. T., Si, B., Kang, X., et al. (2019). Experimental and model enhancement of food waste hydrothermal liquefaction with combined effects of biochemical composition and reaction conditions. *Bioresour. Technol.* 284, 139–147. doi: 10.1016/j.biortech.2019.03.076

Alhassan, Y., Kumar, N., and Bugaje, I. M. (2016). Hydrothermal liquefaction of de-oiled *Jatropha curcas* cake using Deep Eutectic Solvents (DESs) as catalysts and co-solvents. *Bioresour. Technol.* 199, 375–381. doi: 10.1016/j.biortech.2015.07.116

Al-Wabel, M. I., Rafique, M. I., Ahmad, M., Ahmad, M., Hussain, A., and Usman, A. R. A. (2018). Pyrolytic and hydrothermal carbonization of date palm leaflets: characteristics and ecotoxicological effects on seed germination of lettuce. *Saudi. J. Biol. Sci.* 26, 665–672. doi: 10.1016/j.sjbs.2018.05.017

Anastasakis, K., and Ross, A. B. (2011). Hydrothermal liquefaction of the brown macro-alga laminaria *Saccharina*: effect of reaction conditions on product distribution and composition. *Bioresour. Technol.* 102, 4876–4883. doi: 10.1016/j.biortech.2011.01.031

Anastasakis, K., and Ross, A. B. (2015). Hydrothermal liquefaction of four brown macro-algae commonly found on the UK coasts: an energetic analysis of the process and comparison with bio-chemical conversion methods. *Fuel* 139, 546–553. doi: 10.1016/j.fuel.2014.09.006

Bayat, H., Cheng, F., Dehghanizadeh, M., Soliz, N., Brewer, C. E., and Jena, U. (2019). "Hydrothermal liquefaction of food waste: bio-crude oil characterization, mass and energy balance," in *2019 ASABE Annual International Meeting* (St. Joseph, MI: ASABE). doi: 10.13031/aim.201900974

Bayat, H., Dehghanizadeh, M., Holguin, F. O., Jena, U., and Brewer, C. E. (2020). "Removal of heavy metal ions from wastewater using food waste char," in

2020 ASABE Annual International Virtual Meeting (St. Joseph, MI: ASABE). doi: 10.13031/aim.202001062

Biller, P., and Ross, A. B. (2011). Potential yields and properties of oil from the hydrothermal liquefaction of microalgae with different biochemical content. *Bioresour. Technol.* 102, 215–225. doi: 10.1016/j.biortech.2010.06.028

Blakney, G. T., Hendrickson, C. L., and Marshall, A. G. (2011). Predator data station: a fast data acquisition system for advanced FT-ICR MS experiments. *Int. J. Mass. Spect.* 306, 246–252. doi: 10.1016/j.ijms.2011.03.009

Brown, T. M., Duan, P., and Savage, P. E. (2010). Hydrothermal liquefaction and gasification of *Nannochloropsis* sp. *Energ. Fuels* 24, 3639–3646. doi: 10.1021/ef100203u

Cao, L., Zhang, C., Chen, H., Tsang, D. C. W., Luo, G., Zhang, S., et al. (2017). Hydrothermal liquefaction of agricultural and forestry wastes: state-of-the-art review and future prospects. *Bioresour. Technol.* 245, 1184–1193. doi: 10.1016/j.biortech.2017.08.196

Chen, G.-B., Li, J.-W., Lin, H.-T., Wu, F.-H., and Chao, Y. C. (2018). A study of the production and combustion characteristics of pyrolytic oil from sewage sludge using the Taguchi method. *Energies* 11:2260. doi: 10.3390/en11092260

Chen, G.-B., Li, Y.-H., Lan, C.-H., Lin, H.-T., and Chao, Y.-C. (2017a). Micro-explosion and burning characteristics of a single droplet of pyrolytic oil from castor seeds. *Appl. Thermal. Eng.* 114, 1053–1063. doi: 10.1016/j.applthermaleng.2016.12.052

Chen, W.-H., Lin, Y.-Y., Liu, H.-C., and Baroutian, S. (2020). Optimization of food waste hydrothermal liquefaction by a two-step process in association with a double analysis. *Energy* 199:117438. doi: 10.1016/j.energy.2020.117438

Chen, W.-H., Lin, Y.-Y., Liu, H.-C., Chen, T.-C., Hung, C.-H., Chen, C.-H., et al. (2019a). A comprehensive analysis of food waste derived liquefaction bio-oil properties for industrial application. *Appl. Energy* 237, 283–291. doi: 10.1016/j.apenergy.2018.12.084

Chen, W.-H., Lin, Y.-Y., Liu, H.-C., Chen, T.-C., Hung, H.-C., and Chen, C.-H. (2019b). Analysis of physicochemical properties of liquefaction bio-oil from food waste. *Energy Procedia* 158, 61–66. doi: 10.1016/j.egypro.2019.01.036

Chen, W.-T., Qian, W., Zhang, Y., Mazur, Z., Kuo, C.-T., Scheppe, K., et al. (2017b). Effect of ash on hydrothermal liquefaction of high-ash content algal biomass. *Algal. Res.* 25, 297–306. doi: 10.1016/j.algal.2017.05.010

Chen, W.-T., Zhang, Y., Zhang, J., Schideman, L., Yu, G., Zhang, P., et al. (2014). Co-liquefaction of swine manure and mixed-culture algal biomass from a wastewater treatment system to produce bio-crude oil. *Appl. Energy* 128, 209–216. doi: 10.1016/j.apenergy.2014.04.068

Chen, X., Ma, X., Chen, L., Lu, X., and Tian, Y. (2020). Hydrothermal liquefaction of *Chlorella pyrenoidosa* and effect of emulsification on upgrading the bio-oil. *Bioresour. Technol.* 316:123914. doi: 10.1016/j.biortech.2020.123914

Cheng, F., Bayat, H., Jena, U., and Brewer, C. E. (2020a). Impact of feedstock composition on pyrolysis of low-cost, protein-and lignin-rich biomass: a review. *J. Anal. Appl. Pyrolysis* 147:104780. doi: 10.1016/j.jaap.2020.104780

Cheng, F., Cui, Z., Chen, L., Jarvis, J., Paz, N., Schaub, T., et al. (2017). Hydrothermal liquefaction of high- and low-lipid algae: Bio-crude oil chemistry. *Appl. Energy* 206, 278–292. doi: 10.1016/j.apenergy.2017.08.105

Cheng, F., Cui, Z., Mallick, K., Nirmalakhandan, N., and Brewer, C. E. (2018). Hydrothermal liquefaction of high- and low-lipid algae: mass and energy balances. *Bioresour. Technol.* 258, 158–167. doi: 10.1016/j.biortech.2018.02.100

Cheng, F., Dehghanizadeh, M., Audu, M. A., Jarvis, J. M., Holguin, F. O., and Brewer, C. E. (2020b). Characterization and evaluation of guayule processing residues as potential feedstock for biofuel and chemical production. *Indust. Crops. Prod.* 150:112311. doi: 10.1016/j.indcrop.2020.112311

Cheng, F., Mallick K, Gedara, Sh. M. H., Jarvis, J. M., Schaub, T., Jena, U., Nirmalakhandan, N., and Brewer, C. E. (2019). Hydrothermal liquefaction of Galdieria sulphuraria grown on municipal wastewater. *Bioresour. Technol.* 292:121884. doi: 10.1016/j.biortech.2019.121884

Cheng, F., Tompsett, G. A., Murphy, C. M., Maag, A. R., Carabillo, N., Bailey, M., et al. (2020c). Synergistic effects of inexpensive mixed metal oxides for catalytic hydrothermal liquefaction of food wastes. *ACS Sustain. Chem. Eng.* 8, 6877–6886. doi: 10.1021/acssuschemeng.0c02059

Cheng, S., D'cruz, I., Wang, M., Leitch, M., and Xu, C. (2010). Highly efficient liquefaction of woody biomass in hot-compressed alcohol–water co-solvents. *Energ Fuels* 24, 4659–4667. doi: 10.1021/ef901218w

Christensen, P. R., Mørup, A. J., Mamakhel, A., Glasius, M., Becker, J., and Iversen, B. B. (2014). Effects of heterogeneous catalyst in hydrothermal liquefaction of dried distillers grains with solubles. *Fuel* 123, 158–166. doi: 10.1016/j.fuel.2014.01.037

Corilo, Y. E. (2014). *PetroOrg Software*. Tallahassee, FL: Florida State University.

Dandamudi, K. P. R., Muhammed Luboowa, K., Laideson, M., Murdock, T., Seger, M., McGowen, J., et al. (2020). Hydrothermal liquefaction of *Cyanidioschyzon merolae* and *Salicornia bigelovii* Torr.: the interaction effect on product distribution and chemistry. *Fuel* 277:118146. doi: 10.1016/j.fuel.2020.118146

Déniel, M., Haarlemmer, G., Roubaud, A., Weiss-Hortala, E., and Fages, J. (2016). Energy valorisation of food processing residues and model compounds by hydrothermal liquefaction. *Renew. Sustain. Energ. Rev.* 54, 1632–1652. doi: 10.1016/j.rser.2015.10.017

Duan, P., and Savage, P. E. (2011). Hydrothermal liquefaction of a microalga with heterogeneous catalysts. *Indust. Eng. Chem. Res.* 50, 52–61. doi: 10.1021/ie100758s

EngineeringToolBox (2003). *Fuels and Chemicals—Autoignition Temperatures*. Available online at: https://www.engineeringtoolbox.com/fuels-ignition-temperatures-d_171.html (accessed December 10, 2020).

Folch, J., Lees, M., and Stanley, G. H. S. (1957). A simple method for the isolation and purification of total lipides from animal tissues. *J. Biol. Chem.* 226, 497–509. doi: 10.1016/S0021-9258(18)64849-5

Gai, C., Zhang, Y., Chen, W.-T., Zhang, P., and Dong, Y. (2014). Energy and nutrient recovery efficiencies in biocrude oil produced via hydrothermal liquefaction of *Chlorella pyrenoidosa*. *RSC Adv.* 4, 16958–16967. doi: 10.1039/c3ra46607h

Gai, C., Zhang, Y., Chen, W.-T., Zhang, P., and Dong, Y. (2015). An investigation of reaction pathways of hydrothermal liquefaction using *Chlorella pyrenoidosa* and *Spirulina platensis*. *Energ. Conv. Manage.* 96, 330–339. doi: 10.1016/j.enconman.2015.02.056

Gollakota, A. R. K., Kishore, N., and Gu, S. (2018). A review on hydrothermal liquefaction of biomass. *Renew. Sustain. Energ. Rev.* 81, 1378–1392. doi: 10.1016/j.rser.2017.05.178

Gu, Y., Zhang, X., Deal, B., Han, L., Zheng, J., and Ben, H. (2019). Advances in energy systems for valorization of aqueous byproducts generated from hydrothermal processing of biomass and systems thinking. *Green. Chem.* 21, 2518–2543. doi: 10.1039/C8GC03611J

Gunders, D., and Bloom, J. (2017). *Wasted: How America Is Losing Up to 40 Percent of Its Food From Farm to Fork to Landfill*. New York, NY: Natural Resources Defense Council.

Hames, B., Scarlata, C., and Sluiter, A. (2008). *Determination of Protein Content in Biomass*. Golden, CO: National Renewable Energy Laboratory.

Hassan, M. A., Yee, L.-N., Yee, P. L., Ariffin, H., Raha, A. R., Shirai, Y., et al. (2013). Sustainable production of polyhydroxyalkanoates from renewable oil-palm biomass. *Biomass Bioenerg.* 50, 1–9. doi: 10.1016/j.biombioe.2012.10.014

Heldman, D. R. (2001). "Prediction models for thermophysical properties of foods," in *Food Processing Operation Modeling: Design and Analysis, 2nd Edn.,* ed J. Irudayaraj (New Brunswick, NJ: CRC Press), 1–24. doi: 10.1201/9780203908105.ch1

Hongthong, S., Leese, H. S., and Chuck, C. J. (2020). Valorizing plastic-contaminated waste streams through the catalytic hydrothermal processing of polypropylene with lignocellulose. *ACS Omega* 5, 20586–20598. doi: 10.1021/acsomega.0c02854

Islam, M. A., Limon, M. S. H., Romić, M., and Islam, M. A. (2021). Hydrochar-based soil amendments for agriculture: a review of recent progress. *Arab. J. Geosci.* 14:102. doi: 10.1007/s12517-020-06358-8

Jarvis, J. M., Billing, J. M., Hallen, R. T., Schmidt, A. J., and Schaub, T. M. (2017). Hydrothermal liquefaction biocrude compositions compared to petroleum crude and shale oil. *Energ. Fuels* 31, 2896–2906. doi: 10.1021/acs.energyfuels.6b03022

Jena, U., Das, K. C., and Kastner, J. R. (2011). Effect of operating conditions of thermochemical liquefaction on biocrude production from *Spirulina platensis*. *Bioresour. Technol.* 102, 6221–6229. doi: 10.1016/j.biortech.2011.02.057

Jian-yuan, C., and Xue-xing, S. (1987). Determination of the devolatilization index and combustion characteristic index of pulverized coals. *Power. Eng.* 7, 33–36.

Kaiser, N. K., Quinn, J. P., Blakney, G. T., Hendrickson, C. L., and Marshall, A. G. (2011). A novel 9.4 Tesla FTICR mass spectrometer with improved sensitivity, mass resolution, and mass range. *J. Amer. Soc. Mass. Spect.* 22, 1343–1351. doi: 10.1007/s13361-011-0141-9

Kapusta, K. (2018). Effect of ultrasound pretreatment of municipal sewage sludge on characteristics of bio-oil from hydrothermal liquefaction process. *Waste Manage.* 78, 183–190. doi: 10.1016/j.wasman.2018.05.043

Kendrick, E. (1963). A mass scale based on CH2= 14.0000 for high resolution mass spectrometry of organic compounds. *Anal. Chem.* 35, 2146–2154. doi: 10.1021/ac60206a048

Kim, S., Kramer, R. W., and Hatcher, P. G. (2003). Graphical method for analysis of ultrahigh-resolution broadband mass spectra of natural organic matter, the van krevelen diagram. *Anal. Chem.* 75, 5336–5344. doi: 10.1021/ac034415p

Kostyukevich, Y., Vlaskin, M., Borisova, L., Zherebker, A., Perminova, I., Kononikhin, A., et al. (2018). Investigation of bio-oil produced by hydrothermal liquefaction of food waste using ultrahigh resolution Fourier transform ion cyclotron resonance mass spectrometry. *Eur. J. Mass. Spectrom.* 24, 116–123. doi: 10.1177/1469066717737904

Ledford, E. B., Rempel, D. L., and Gross, M. L. (1984). Space charge effects in Fourier transform mass spectrometry. II. Mass calibration. *Anal. Chem.* 56, 2744–2748. doi: 10.1021/ac00278a027

León, M., Marcilla, A. F., and García, Á. N. (2019). Hydrothermal liquefaction (HTL) of animal by-products: influence of operating conditions. *Waste Manage.* 99, 49–59. doi: 10.1016/j.wasman.2019.08.022

Leonardis, I., Chiaberge, S., Fiorani, T., Spera, S., Battistel, E., Bosetti, A., et al. (2013). Characterization of bio-oil from hydrothermal liquefaction of organic waste by NMR spectroscopy and FTICR mass spectrometry. *ChemSusChem* 6, 160–167. doi: 10.1002/cssc.201200314

Leow, S., Witter, J. R., Vardon, D. R., Sharma, B. K., Guest, J. S., and Strathmann, T. J. (2015). Prediction of microalgae hydrothermal liquefaction products from feedstock biochemical composition. *Green. Chem.* 17, 3584–3599. doi: 10.1039/C5GC00574D

Li, B., Feng, S. H., Niasar, H. S., Zhang, Y. S., Yuan, Z. S., Schmidt, J., et al. (2016). Preparation and characterization of bark-derived phenol formaldehyde foams. *RSC. Adv.* 6, 40975–40981. doi: 10.1039/C6RA05392K

Li, L., Diederick, R., Flora, J. R. V., and Berge, N. D. (2013). Hydrothermal carbonization of food waste and associated packaging materials for energy source generation. *Waste Manage.* 33, 2478–2492. doi: 10.1016/j.wasman.2013.05.025

Lu, J., Li, H., Zhang, Y., and Liu, Z. (2018). Nitrogen migration and transformation during hydrothermal liquefaction of livestock manures. *ACS Sus. Chem. Eng.* 6, 13570–13578. doi: 10.1021/acssuschemeng.8b03810

Lu, J., Zhang, J., Zhu, Z., Zhang, Y., Zhao, Y., Li, R., et al. (2017). Simultaneous production of biocrude oil and recovery of nutrients and metals from human feces via hydrothermal liquefaction. *Energ. Convers. Manag.* 134, 340–346. doi: 10.1016/j.enconman.2016.12.052

Lu, J.-J., and Chen, W.-H. (2015). Investigation on the ignition and burnout temperatures of bamboo and sugarcane bagasse by thermogravimetric analysis. *Appl. Energ.* 160, 49–57. doi: 10.1016/j.apenergy.2015.09.026

Maag, A., Paulsen, A., Amundsen, T., Yelvington, P., Tompsett, G., and Timko, M. (2018). Catalytic hydrothermal liquefaction of food waste using CeZrOx. *Energies* 11:564. doi: 10.3390/en11030564

Madsen, R. B., and Glasius, M. (2019). How do hydrothermal liquefaction conditions and feedstock type influence product distribution and elemental composition? *Indust. Eng. Chem. Res.* 58, 17583–17600. doi: 10.1021/acs.iecr.9b02337

Marx, S., Venter, R., Karmee, S. K., Louw, J., and Truter, C. (2020). Biofuels from spent coffee grounds: comparison of processing routes. *Biofuels* 1–7. doi: 10.1080/17597269.2020.1793538

Masmoudi, M., Besbes, S., Chaabouni, M., Robert, C., Paquot, M., Blecker, C., et al. (2008). Optimization of pectin extraction from lemon by-product with acidified date juice using response surface methodology. *Carbohydr. Polym.* 74, 185–192. doi: 10.1016/j.carbpol.2008.02.003

Matayeva, A., Bianchi, D., Chiaberge, S., Cavani, F., and Basile, F. (2019). Elucidation of reaction pathways of nitrogenous species by hydrothermal liquefaction process of model compounds. *Fuel* 240, 169–178. doi: 10.1016/j.fuel.2018.11.136

Motavaf, B., and Savage, P. E. (2021). Effect of process variables on food waste valorization via hydrothermal liquefaction. *ACS ES&T Eng.* 3, 363–374. doi: 10.1021/acsestengg.0c00115

Nawaz, H., Shi, J., Mittal, G. S., and Kakuda, Y. (2006). Extraction of polyphenols from grape seeds and concentration by ultrafiltration. *Sep. Purif. Technol.* 48, 176–181. doi: 10.1016/j.seppur.2005.07.006

Niu, S.-l., Han, K.-h., and Lu, C.-m. (2011). Characteristic of coal combustion in oxygen/carbon dioxide atmosphere and nitric oxide release during this process. *Energ. Convers. Manag.* 52, 532–537. doi: 10.1016/j.enconman.2010.07.028

Obeid, R., Lewis, D. M., Smith, N., Hall, T., and van Eyk, P. (2020). Reaction kinetics and characterisation of species in renewable crude from hydrothermal liquefaction of monomers to represent organic fractions of biomass feedstocks. *Chem. Eng. J.* 389:124397. doi: 10.1016/j.cej.2020.124397

Palacio Lozano, D. C., Ramírez, C. X., Sarmiento Chaparro, J. A., Thomas, M. J., Gavard, R., Jones, H. E., et al. (2020). Characterization of bio-crude components derived from pyrolysis of soft wood and its esterified product by ultrahigh resolution mass spectrometry and spectroscopic techniques. *Fuel* 259:116085. doi: 10.1016/j.fuel.2019.116085

Palardy, O., Behnke, C., and Laurens, L. M. L. (2017). Fatty amide determination in neutral molecular fractions of green crude hydrothermal liquefaction oils from algal biomass. *Energ Fuels* 31, 8275–8282. doi: 10.1021/acs.energyfuels.7b01175

Pavlovic, I., Knez, Z., and Skerget, M. (2013). Hydrothermal reactions of agricultural and food processing wastes in sub-and supercritical water: a review of fundamentals, mechanisms, and state of research. *J. Agric. Food. Chem.* 61, 8003–8025. doi: 10.1021/jf401008a

Peterson, A. A., Vogel, F., Lachance, R. P., Fröling, M., Antal, M. J., and Tester, J. W. (2008). Thermochemical biofuel production in hydrothermal media: a review of sub-and supercritical water technologies. *Energy Environ. Sci.* 1:32. doi: 10.1039/b810100k

Pham, T. P. T., Kaushik, R., Parshetti, G. K., Mahmood, R., and Balasubramanian, R. (2015). Food waste-to-energy conversion technologies: current status and future directions. *Waste Manage.* 38, 399–408. doi: 10.1016/j.wasman.2014.12.004

Posmanik, R., Martinez, C. M., Cantero-Tubilla, B., Cantero, D. A., Sills, D. L., Cocero, M. J., et al. (2017). Acid and alkali catalyzed hydrothermal liquefaction of dairy manure digestate and food waste. *ACS Sus. Chem. Eng.* 6, 2724–2732. doi: 10.1021/acssuschemeng.7b04359

Promdej, C., and Matsumura, Y. (2011). Temperature effect on hydrothermal decomposition of glucose in sub- and supercritical water. *Ind. Eng. Chem. Res.* 50, 8492–8497. doi: 10.1021/ie200298c

Qambrani, N., Rahman, M., Won, S., Shim, S., and Ra, C. (2017). Biochar properties and eco-friendly applications for climate change mitigation, waste management, and wastewater treatment: a review. *Renew. Sus. Energ. Rev.* 79, 255–273. doi: 10.1016/j.rser.2017.05.057

Qiu, Y., Aierzhati, A., Cheng, J., Guo, H., Yang, W., and Zhang, Y. (2019). Biocrude oil production through the maillard reaction between leucine and glucose during hydrothermal liquefaction. *Energy Fuels* 33, 8758–8765. doi: 10.1021/acs.energyfuels.9b01875

Ren, X., Meng, J., Moore, A. M., Chang, J., Gou, J., and Park, S. (2014). Thermogravimetric investigation on the degradation properties and combustion performance of bio-oils. *Bioresour. Technol.* 152, 267–274. doi: 10.1016/j.biortech.2013.11.028

Savory, J. J., Kaiser, N. K., McKenna, A. M., Xian, F., Blakney, G. T., Rodgers, R. P., et al. (2011). Parts-per-billion fourier transform ion cyclotron resonance mass measurement accuracy with a "walking" calibration equation. *Anal. Chem.* 83, 1732–1736. doi: 10.1021/ac102943z

Shakya, R., Whelen, J., Adhikari, S., Mahadevan, R., and Neupane, S. (2015). Effect of temperature and Na_2CO_3 catalyst on hydrothermal liquefaction of algae. *Algal. Res.* 12, 80–90. doi: 10.1016/j.algal.2015.08.006

Shi, Q., Hou, D., Chung, K. H., Xu, C., Zhao, S., and Zhang, Y. (2010). Characterization of heteroatom compounds in a crude oil and its saturates, aromatics, resins, and asphaltenes (SARA) and non-basic nitrogen fractions analyzed by negative-ion electrospray ionization fourier transform ion cyclotron resonance mass spectrometry. *Energ Fuels* 24, 2545–2553. doi: 10.1021/ef901564e

Simoneit, B. R. T., Rushdi, A. I., bin Abas, M. R., and Didyk, B. M. (2003). Alkyl amides and nitriles as novel tracers for biomass burning. *Environ. Sci. Technol.* 37, 16–21. doi: 10.1021/es020811y

Sluiter, A., Hames, B., Ruiz, R., Scarlata, C., Sluiter, J., Templeton, D., et al. (2008). "Determination of structural carbohydrates and lignin in biomass," in *Laboratory Analytical Procedure* (Golden, CO: National Renewable Energy Laboratory), 1–16.

Snowden-Swan, L. J., Zhu, Y., Jones, S. B., Elliott, D. C., Schmidt, A. J., Hallen, R. T., et al. (2016). *Hydrothermal Liquefaction and Upgrading of Municipal Wastewater Treatment Plant Sludge: A Preliminary Techno-Economic Analysis, Rev. 1.* Richland, WA: Pacific Northwest National Lab (PNNL). doi: 10.2172/1327165

Sowbhagya, H. B., and Chitra, V. N. (2010). Enzyme-assisted extraction of flavorings and colorants from plant materials. *Crit. Rev. Food. Sci. Nutr.* 50, 146–161. doi: 10.1080/10408390802248775

Stanford, L. A., Kim, S., Rodgers, R. P., and Marshall, A. G. (2006). Characterization of compositional changes in vacuum gas oil distillation cuts by electrospray ionization Fourier transform– ion cyclotron resonance (FT–ICR) mass spectrometry. *Energy Fuels* 20, 1664–1673. doi: 10.1021/ef060104g

Sudasinghe, N., Dungan, B., Lammers, P., Albrecht, K., Elliott, D., Hallen, R., et al. (2014). High resolution FT-ICR mass spectral analysis of bio-oil and residual water soluble organics produced by hydrothermal liquefaction of the marine microalga Nannochloropsis salina. *Fuel* 119, 47–56. doi: 10.1016/j.fuel.2013.11.019

Tang, X., Zhang, C., and Yang, X. (2019). Hydrothermal liquefaction of model compounds protein and glucose: effect of maillard reaction on low lipid microalgae. *IOP Confer. Ser. Mater. Sci. Eng.* 611:012026. doi: 10.1088/1757-899X/611/1/012026

Tekin, K., Akalin, M. K., and Karagöz, S. (2016). The effects of water tolerant Lewis acids on the hydrothermal liquefaction of lignocellulosic biomass. *J. Energy Inst.* 89, 627–635. doi: 10.1016/j.joei.2015.06.003

Tian, C., Liu, Z., Zhang, Y., Li, B., Cao, W., Lu, H., et al. (2015). Hydrothermal liquefaction of harvested high-ash low-lipid algal biomass from Dianchi lake: effects of operational parameters and relations of products. *Bioresourc. Technol.* 184, 336–343. doi: 10.1016/j.biortech.2014.10.093

Tognotti, L., Malotti, A., Petarca, L., and Zanelli, S. (1985). Measurement of ignition temperature of coal particles using a thermogravimetric technique. *Combust. Sci. Technol.* 44, 15–28. doi: 10.1080/00102208508960290

U.S.E.P.A. (2020a). *Inventory of US Greenhouse Gas Emissions and Sinks: 1990–2018.* ed E. 430-F-20-002. Washington, DC.

U.S.E.P.A. (2020b). *Advancing Sustainable Materials Management: 2018 Fact Sheet Assessing Trends in Materials Generation and Management in the United States.* Washington, DC.

Vahur, S., Teearu, A., Haljasorg, T., Burk, P., Leito, I., and Kaljurand, I. (2012). Analysis of dammar resin with MALDI-FT-ICR-MS and APCI-FT-ICR-MS. *J. Mass. Spectrom.* 47, 392–409. doi: 10.1002/jms.2971

Vardon, D. R., Sharma, B. K., Blazina, G. V., Rajagopalan, K., and Strathmann, T. J. (2012). Thermochemical conversion of raw and defatted algal biomass via hydrothermal liquefaction and slow pyrolysis. *Bioresour. Technol.* 109, 178–187. doi: 10.1016/j.biortech.2012.01.008

Vardon, D. R., Sharma, B. K., Scott, J., Yu, G., Wang, Z., Schideman, L., et al. (2011). Chemical properties of biocrude oil from the hydrothermal liquefaction of Spirulina algae, swine manure, and digested anaerobic sludge. *Bioresour. Technol.* 102, 8295–8303. doi: 10.1016/j.biortech.2011.06.041

Viganó, J., Machado, A. P. d. F., and Martínez, J. (2015). Sub- and supercritical fluid technology applied to food waste processing. *J. Supercrit. Fluids* 96, 272–286. doi: 10.1016/j.supflu.2014.09.026

Wang, L., Xiu, S., and Shahbazi, A. (2016). Combustion characteristics of bio-oil from swine manure/crude glycerol co-liquefaction by thermogravimetric analysis technology. *Energy Sources Part A Recov Utilization Environ. Effects* 38, 2250–2257. doi: 10.1080/15567036.2011.618819

Wang, X., Chen, Q., and Lü, X. (2014). Pectin extracted from apple pomace and citrus peel by subcritical water. *Food Hydrocolloids* 38, 129–137. doi: 10.1016/j.foodhyd.2013.12.003

Watson, J., Wang, T., Si, B., Chen, W.-T., Aierzhati, A., and Zhang, Y. (2020). Valorization of hydrothermal liquefaction aqueous phase: pathways towards commercial viability. *Prog. Energy Combust. Sci.* 77:100819. doi: 10.1016/j.pecs.2019.100819

Wu, B., Berg, S. M., Remucal, C. K., and Strathmann, T. J. (2020). Evolution of N-containing compounds during hydrothermal liquefaction of sewage sludge. *ACS Sus. Chem. Eng.* 8, 18303–18313. doi: 10.1021/acssuschemeng.0c07060

Xu, D., Lin, G., Liu, L., Wang, Y., Jing, Z., and Wang, S. (2018). Comprehensive evaluation on product characteristics of fast hydrothermal liquefaction of sewage sludge at different temperatures. *Energy* 159, 686–695. doi: 10.1016/j.energy.2018.06.191

Yuan, C., Emelianov, D. A., and Varfolomeev, M. A. (2018). Oxidation behavior and kinetics of light, medium, and heavy crude oils characterized by thermogravimetry coupled with fourier transform infrared spectroscopy. *Energy Fuels* 32, 5571–5580. doi: 10.1021/acs.energyfuels.8b00428

Zastrow, D. J., and Jennings, P. A. (2013). "Hydrothermal liquefaction of food waste and model food waste compounds," in *American Institute of Chemical Engineers (AIChE) 2013 Annual Meeting* (San Francisco, CA).

Zhang, Y., Arnold, R., Paavola, T., Vaz, F., Neiva Correia, C., Cavinato, C., et al. (2013). "Compositional analysis of food waste entering the source segregation stream in four European regions and implications for valorisation via anaerobic digestion," in *Sardinia 2013 14th International Waste Management and Landfill Symposium* (Sardinia).

Zhang, Y., Minaret, J., Yuan, Z., Dutta, A., and Xu, C. (2018). Mild hydrothermal liquefaction of high water content agricultural residue for bio-crude oil production: a parametric study. *Energies* 11:3129. doi: 10.3390/en11113129

Zhou, D., Zhang, L., Zhang, S., Fu, H., and Chen, J. (2010). Hydrothermal liquefaction of macroalgae Enteromorpha prolifera to bio-oil. *Energy Fuels* 24, 4054–4061. doi: 10.1021/ef100151h

Zhu, Z., Si, B., Lu, J., Watson, J., Zhang, Y., and Liu, Z. (2017). Elemental migration and characterization of products during hydrothermal liquefaction of cornstalk. *Bioresour. Technol.* 243, 9–16. doi: 10.1016/j.biortech.2017.06.085

Zhu, Z., Toor, S. S., Rosendahl, L., and Chen, G. (2014). Analysis of product distribution and characteristics in hydrothermal liquefaction of barley straw in subcritical and supercritical water. *Environ. Prog. Sus. Energy* 33, 737–743. doi: 10.1002/ep.11977

Conflict of Interest: The authors declare that the research was conducted in the absence of any commercial or financial relationships that could be construed as a potential conflict of interest.